Magnetic and Electronic studies on $Cr_{100-x}Ir_x$ alloy single crystals

P R Fernando, A R E Prinsloo and C J Sheppard

Department of Physics, University of Johannesburg, PO Box 524, Auckland Park, 2006

Author e-mail address: alettap@uj.ac.za

Abstract. An investigation of the physical properties of $Cr_{100-x}Ir_x$ alloy single crystals, with x = 0.07, 0.15, 0.20 and 0.25, were previously used to establish the magnetic phase diagram of $Cr_{100-x}Ir_x$ alloy system around triple point concentration where the various magnetic phases co-exist. The present study extends these results by considering the temperature (T) dependence of the Seebeck coefficient (S), specific heat (C_p) and Hall coefficient (R_H) measurements, in addition to the electrical resistivity (ρ). Well defined anomalies were observed in the $\rho(T)$ and $S(T)$ curves of all the samples, except x = 0.25 alloy in $S(T)$ curve which is above 380 K (T_N = 391.5 K). The anomaly is the effect of an antiferromagnetic to paramagnetic phase transition on heating through the Néel temperature (T_N). Contrary to what is normally expected, it is noted that the anomaly related to T_N is more prominent in the $\rho(T)$ curves than in the $S(T)$ curves. R_H measurements carried out from 360 K down to 2 K in a constant magnetic field of 6 T, shows only weak anomalies at T_N for certain samples. The electronic Sommerfeld coefficient (γ), obtained from the low temperature C_p/T versus T^2 data, fits in well with the γ versus electron-to-atom (e/a) ratio curve previously published for certain Cr alloys.

1. Introduction

The electron and hole Fermi surfaces of pure Cr and its alloys nest on cooling through the Néel temperature (T_N), resulting in the formation of the spin-density-wave (SDW) when the antiferromagnetic (AFM) phase is entered. This nesting decreases the energy of the system through electron-hole pair condensation and results in the appearance of SDW energy gaps at the Fermi surface in certain directions in k-space [1].

The first parameter of importance in influencing the formation of the SDW is the effect of electron concentration on the area of the electron and hole Fermi surface sheets that nest [1]. The nesting area, and concomitantly the stability of the SDW state, depend on the electron concentration per atom (e/a) which can easily be tuned by alloying Cr (e/a = 6) with group-8 non-magnetic transition metals to increase or decrease the electron concentration [1].

Cr alloys with group-8 non-magnetic transition metals Ru, Os, Rh, Ir and Pt show large anomalies of magnetic origin at the phase transition temperatures [1]. The addition of very small amount of these impurities is enough to introduce phase changes in the magnetic state in the Cr alloys. Furthermore, the magnetic phase diagrams of the Cr alloys with group-8 non-magnetic transition metals contain the commensurate (C) SDW phase, the incommensurate (I) SDW phase, the transverse (T) incommensurate (I) SDW, longitudinal (L) ISDW phases as well as the paramagnetic (P) phase. The

magnetic phase diagrams of these alloys contain a triple point, where the ISDW, CSDW and P phases co-exist [1]. For impurity concentrations (x) below the triple point concentration (x_L), the LISDW, TISDW and P phases are observed, while for $x > x_L$ CSDW phase is observed. The spin-flip transition (T_{SF}) and the Néel transition (T_N) are known as first order phase transitions and the ISDW-CSDW phase transition (T_{IC}) are second order in nature [1, 2].

The Cr-Ir single crystals used in this study were also previously investigated using electrical resistivity, ultrasonic attenuation, thermal expansion and magnetoelastic measurements [3-5]. In order to extend these investigations and draw new correlations between the various physical properties, electrical resistivity (ρ), Seebeck coefficient (S), specific heat (C_p) and Hall coefficient (R_H) measurements were done in the present study.

2. Experimental

The $Cr_{100-x}Ir_x$ single crystals, with x = 0.07, 0.15, 0.20 and 0.25, were prepared using the floating-zone technique [3-5] and previously investigated using different measurement techniques [3-5]. In the present study electrical resistivity $\rho(T)$ in the temperature (T) range 2 K $\leq T \leq$ 630 K, Seebeck coefficient $S(T)$, specific heat $C_p(T)$ measurements were done in the temperature range 2 K $\leq T \leq$ 380 K and Hall coefficient (R_H) were carried out in the same temperature range as $C_p(T)$ and at a constant magnetic field of 6 T using a Quantum Design (QD) Physical Property Measurement System (PPMS). All these measurements were performed along the cubic [100] direction. The electrical resistivity measurements were done during heating and cooling.

3. Results and Discussion

Figure 1(a) shows electrical resistivity (ρ) as a function of temperature (T) in the range 2 K $\leq T \leq$ 630 K. Well defined anomalies in the form of clear minima followed by prominent domes are observed near Néel temperature (T_N) on cooling through the ISDW-P region. T_N and the size of the dome increase with increasing the Ir concentration, x. This anomalous behaviour is associated with the formation of the SDW on entering the antiferromagnetic phase on cooling through the Néel temperature (T_N) [1]. T_N is often defined for Cr and its dilute alloys as the temperature associated with the minimum in $d\rho/dT$ accompanying the magnetic phase transition [1]. This definition was also used in the present study and an example is shown in Figure 1(b). Present results are in good agreement with previous results of the electrical resistivity measurements on single and polycrystalline $Cr_{100-x}Ir_x$ alloys [5-10]. Thermal hysteresis was observed during heating (T_{IC}) and cooling (T_{CI}) in $Cr_{99.80}Ir_{0.20}$ single crystal, but the temperature range varies slightly from that previously observed [5].

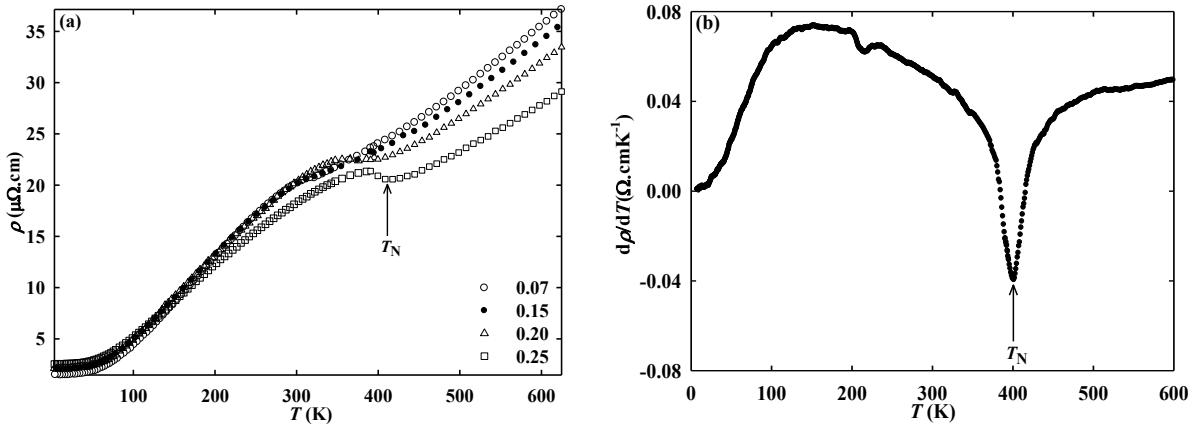

Figure 1. (a) Electrical resistivity (ρ) as a function of temperature (T) in the range 2 K $\leq T \leq$ 630 K for the $Cr_{100-x}Ir_x$ single crystals. Symbols for concentrations are indicated in the legend. (b) $d\rho/dT$ as a function of temperature (T) for x = 0.25 sample. The minimum is used to indicate the Néel temperature, T_N.

The Seebeck coefficient (S) of $Cr_{100-x}Ir_x$ alloys were measured as a function of temperature (T) in the range 2 K ≤ T ≤ 380 K. Figure 2 shows $S(T)$ curves for alloys, with x = 0.07 and 0.20. The S versus T curve for 0.07 at.% Ir, shows a well-defined anomaly with prominent dome associated with T_N, around the same temperature region in which the electrical resistivity shows similar anomaly. T_N for 0.25 at.% Ir lies above the measured temperature range 2 K ≤ T ≤ 380 K and this cannot be seen in the curve. This T_N was calculated from the derivative of d$S(T)$/dT accompanying the $S(T)$ magnetic anomaly, which is indicated by an arrow in Figure 2.

The value of T_N, as well as the magnitude of the dome in $S(T)$ increases with x and its position shifts to higher temperatures. The T_N values obtained from $\rho(T)$ and $S(T)$ in the present studies are approximately equal to the previous studies. The formation of dome in $\rho(T)$ and $S(T)$ are due to the formation of the SDW resulting in the formation of additional energy gaps in band structure of Cr-alloys [1, 5]. Using the experimental electrical resistivity and Seebeck coefficient results, the energy gap (ΔE_g), can be calculated using the equation, $E_g = \frac{\pi^2 {k_B}^2 T}{3e}\left(\frac{\rho}{\rho}\right)^2 \frac{1}{S}$ [11]. Here ρ is the total electrical resistivity, $\Delta\rho$ is the extrapolated resistivity, ΔS is the extrapolated Seebeck coefficient at temperature T. The quantity $\Delta\rho$ and ΔS are the difference between the maximum value of ρ and S in the antiferromagnetic region and the extrapolated resistivity and Seebeck coefficient value from the paramagnetic region at the same temperature. The Fermi energy, ΔE_g, was calculated for x = 0.07, which is equal to 0.1 meV.

The electronic Sommerfeld coefficient, γ, was determined for the single crystals by fitting the low temperature specific heat data to the equation $C_p/T = \gamma + \beta T^2$, where γ is the electronic Sommerfeld coefficient related to density of state, $n(E_F)$, and β is the lattice contribution related to Debye temperature θ_D. The experimental data points in the C_p/T versus T^2 curve was well fitted by least-squares linear fits, which is a straight line in the temperature range 2 K ≤ T^2 ≤ 7 K for all $Cr_{100-x}Ir_x$ single crystals. The inset in Figure 3 shows such a fit for the x = 0.20 sample as an example. The calculated gradients for the C_p/T versus T^2 curves for all the single crystals in the range T^2 ≤ 5.5 K is approximately equal to the gradients obtained for 4 ≤ T^2 ≤ 400 K.

The values of γ for the $Cr_{100-x}Ir_x$ single crystals is compared with previously studied alloys, such as Cr-V (▼) [13] and (▲) [14], Cr-Re [□] [15, 16], Cr-Ru [◇] [13, 15] alloys in Figure 4. In general these curves show a gradual increase with increasing the e/a ratio of the alloys and started to level off at, e/a = 6.35. Line curves in Figure 4 were plotted by least-squares polynomial fit. The dashed line curves in Figure 4 plotted with the aid of the paramagnetic data points from Cr-V and Cr-Re.

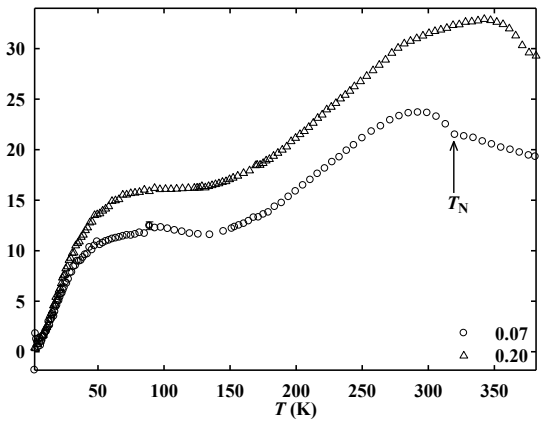

Figure 2. The Seebeck coefficient (S) for $Cr_{100-x}Ir_x$ alloys with x = 0.07 (○) and 0.20 (Δ) as a function of temperature (T) in the range 2 K ≤ T ≤ 380 K.

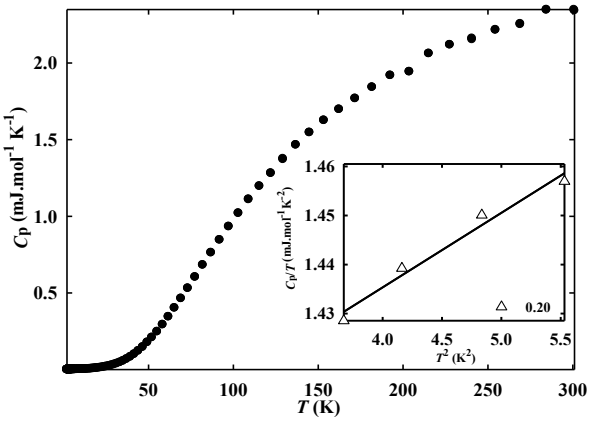

Figure 3. The graph of C_p versus T for 0.25 at.% Ir alloy in the temperature range 2 K ≤ T ≤ 300 K. The inset shows C_p/T versus T^2 for 0.20 at.% Ir alloy, T^2 ≤ 5.5 K. The experimental data points were well fitted using least-squares linear fits.

The curve shows a smooth change in γ in the PM region for Cr-V, in the low region where $e/a \leq 5.95$ and for Cr-Re, in the high diluent region where $e/a \geq 6.25$. For all the AFM alloys all the experimental γ values are suppressed below those observed in the paramagnetic region. This effect is due to the overlapping of the electron and hole Fermi surface sheet and the reduction in the density of states at the Fermi level in the formation of SDW. The γ values of Cr-Ir single crystals are indicated by large open circles in Figure 4, which have approximately similar γ values at $e/a \approx 6.00$. These γ values lie on the dotted curve, which belongs to the alloys Cr-Ru and Cr-Re in the region where $e/a \geq 6.00$ as shown in Figure 4. Therefore, as expected, the Cr-Ir may have the similar trend of Cr-Ru and Cr-Re in high concentration (x), because these alloys are in the same group [1, 2].

Figure 5 illustrates the Hall coefficient of the $Cr_{100-x}Ir_x$ single crystals curves as a function of temperature (T), which shows that the value of $R_H(x)$ at 2 K decreases with increasing the concentration of Ir. $R_H(T)$ curves gradually increase when cooling down to 2 K from 380 K. The single crystal alloys both show a prominent upturn on cooling to $T < T_N$, and the magnitude of the upturn decreases with increasing, x. These effects may be due to an influence of progressive opening up of energy gap due to the SDW in the system. At $T \leq 50$ K the $R_H(T)$ curves levels off, this is attributed to the spin-flip transition (T_{SF}), where the (T) ISDW to (L) ISDW phase transform on cooling [17, 18]. Arrows shown in Figure 5 indicate T_N, T_{SF} and T_{IC} obtained from the work of Martynova *et al.* [3, 5]. The behavioural change in $R_H(T)$ decrease with increasing the concentration, x. This effect may be due to the ISDW to CSDW phase transition around triple point concentration [18] and/or decreasing the number of hole mobility by alloying as well as the domination of the impurity scattering [19].

4. Conclusion

The electrical resistivity $\rho(T)$, Seebeck coefficient $S(T)$, specific heat $C_p(T)$ and Hall measurements $R_H(T)$, of $Cr_{100-x}Ir_x$, with x = 0.07, 0.15, 0.20 and 0.25, single crystals were investigated in the present study. Well defined magnetic anomalies in the form of a hump in the electrical resistivity, $\rho(T)$, curves, show similar trend, compared to previous studies [3-5]. T_N values obtained from $\rho(T)$ and $S(T)$ measurements compare well. However, there is no clear indication for a spin-flip (T_{SF}) transition, previously observed in ultrasonic velocity of sound studies in x = 0.25 crystals in the present study [3]. The γ versus e/a values obtained fits in well with that previously found for other Cr alloys with group-8 diluents [15]. This study can be further expanded as to including $S(T)$, $R_H(T)$ and magnetic susceptibility $\chi(T)$ measurements as a function of temperature for more single crystals for better comparison.

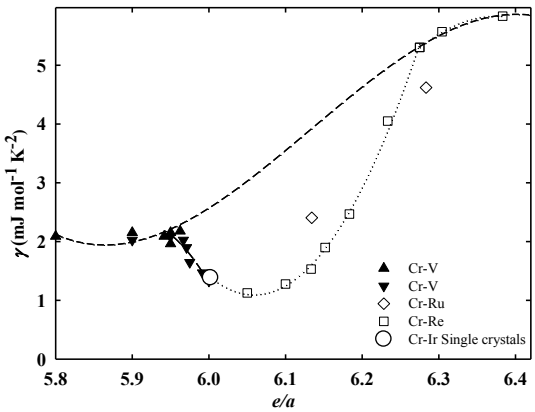

Figure 4. The behaviour of electronic Sommerfeld coefficient (γ) as a function of electron-atom (e/a) ratio for the Cr-V (▼[13] and ▲[14]), Cr-Re (□) [16], Cr-Ru (◇) [13] poly crystals from previous studies redrawn from Heiniger *et al.*[15] and Cr-Ir single crystals [○] from this study. The line curves are guide to eye.

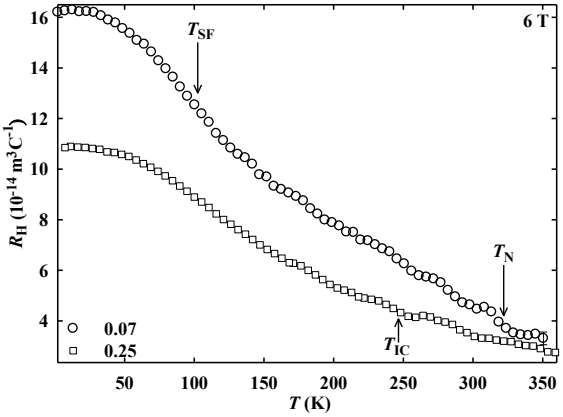

Figure 5. Hall coefficient (R_H) as a function of temperature (T) in the range 2 K $\leq T \leq$ 360 K in a constant applied magnetic field 6 T. The arrows indicate the T_N, T_{SF} and T_{IC}, obtained from the work of Martynova *et al.* [3, 5].

Acknowledgements
This work was supported by the NRF of South Africa under grant numbers 78832 and 61388.

References

[1] Fawcett E, Alberts H L, Galkin V Y, Noakes D R and Yakhmi J V 1994 *Rev. Mod. Phys.* **66** 25.
[2] Fawcett E 1988 *Rev. Mod. Phys.* **60** 209.
[3] Martynova J, Alberts H L and Smit P 1998 *J. Magn. Magn. Mat.* **187** 345.
[4] Martynova J, Alberts H L and Smit P 1998 *J.Phys.:Condens.Matter* **10** 1173.
[5] Martynova J, Alberts H L and Smit P 1996 *J.Phys.:Condens.Matter* **8** 10473.
[6] Fukamichi K and Siato H 1975 *J. Less Common Met.* **40** 357.
[7] Gopalakrishnan I K,Yakhmi J V and Iyer R M 1984 *J. Magn. Magn. Mat.* **46** 207.
[8] Arajs S, Rao K V, Åström H U and De-Young F.Tice 1973 *Physica Scripta.* **8** 109.
[9] Yakhmi J V, Gopalakrishnan I K and Iyer R M 1983 *J. Less Common Met.* **91** 327.
[10] De Young F.Tice, Arajs S and Anderson E E 1971 *Amer. Inst. Phys. Conf. Proc. Magn and Magn. Mat.* **5** 517.
[11] Schröder K and Harry T 1968 *Phys. Kondens. Materie* **7** 318.
[12] Takeuchi J, Sasakura H and Masuda Y 1980 *J. Phys. Soc. Jpn.* **49** 508.
[13] Heiniger F 1966 *Phys. Kondens. Materie* **5** 285.
[14] Cheng C H, Wei C T and Beck P A 1960 *Phys. Rev.* **120(2)** 426.
[15] Heiniger F, Bucher E and Müller J 1966 *Phys. Kondens. Materie* **5** 243.
[16] Muheim J and Müller J 1964 *Phys. Kondens. Materie* **2** 377.
[17] Furuya Y 1976 *J. Phys. Soc. Jpn.* **40** 490.
[18] Sheppard C J, Prinsloo A R E, Alberts H L, Muchono B and Strydom A M 2014 *J. Alloys and Compounds.* **595** 164.
[19] Shabel B S and Schröder K 1967 *J. Phys. Chem. Solids* **28** 2169.